Originally published in *Proceedings of the Fifth International Workshop on Compressible Turbulent Mixing*, ed. R. Young, J. Glimm & B. Boston. ISBN 9810229100, World Scientific (1996).

Vortex Models for Richtmyer–Meshkov Fast/Slow Environments : Scaling Laws for Interface Growth Rates*

N. Zabusky[1], J. Ray[1], and R. S. Samtaney[2]

[1] Department of Mech. and Aero. Eng.
Rutgers University
Piscataway, NJ 08855-0909

[2] Applied Mathematics
California Institute of Technology
Pasadena, CA 91125, USA

Abstract. The *vortex paradigm* [1] provides a cogent physical understanding of the behavior of shock-accelerated density- stratified interfaces at and beyond early times. We use this paradigm to obtain models of the growth rate of a long wavelength perturbation on a planar contact discontinuity.These provide a better agreement with numerical (compressible Euler) simulations over a wider parameter domain than linearized studies e. g. as first conducted by Richtmyer. The domain of our models embraces $1.05 \leq M \leq 4.0$, $1.0 \leq \eta \leq 5.04$ and $A/\lambda = 0.025, 0.05, 0.1$, where M is the Mach number of the incoming planar vertical shock, η is the density ratio across the interface and A/λ is the amplitude to wavelength ratio of the single harmonic perturbation. Our models and scaling laws are extensions of previous works [6], [3] on fast-slow interfaces and apply to the very early, intermediate and late times (when the thin vortex layer "collapses" into a domain of small radius and yields the familiar dipolar vorticity morphology). The models are validated by comparing with simulations of the compressible Euler equations. Agreement is presently within 3 % at low Mach numbers (~ 1.2) and low density ratios ($\eta \sim 3$). The simulations were made with a second order Godunov finite-volume scheme on the CM5 programmed in the SIMD mode.

1 Introduction

A linear stability analysis associated with shocks striking a weak, long–wavelength harmonic perturbation, ($x = A\cos ky, Ak \ll 1$), on an interface between two gases was

*This work was funded in part by a D. O. E. grant, DE-FG02-93ER25179.A000, monitored by Dr. Daniel Hitchcock. The computations were performed on the CM5 at NCSA, University of Illinois, Urbana-Champaign.

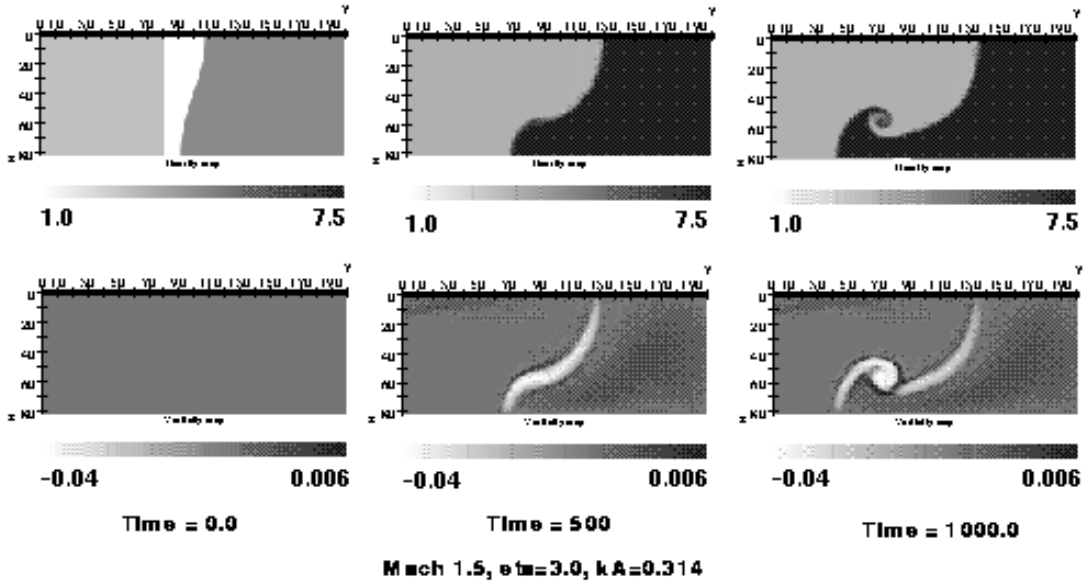

Fig.1 : Density and Vorticity Fields.

done by Richtmyer [2]. He derived linear PDEs for interface dynamics and presented a heuristic "impulsive" formula for amplitude growth rate model

$$\dot{A} = kA|_{0+}\Delta U\frac{\eta - 1}{\eta + 1} \tag{1}$$

where k the wavenumber, η is the density ratio, $A|_{0+}$ is the amplitude of the harmonic, and ΔU is the velocity of the interface from a 1D interaction, after shock passage. Yang, Zhang and Sharp [8] elucidated Richtmyer's linear analysis.

The vortex paradigm is based on the evolution equation in inviscid flows

$$\frac{D\omega}{Dt} = \frac{\nabla\rho \times \nabla p}{\rho^2} + \omega \cdot \nabla\vec{u} - \omega\nabla \cdot \vec{u} \tag{2}$$

As the shock traverses the interface, the misalignment of ∇p and $\nabla\rho$ deposits a vortex sheet on the interface which dominates the largely incompressible evolution of the interface. Due to numerical diffusion, the vortex sheet, over time, becomes a vortex layer (Fig. 1).

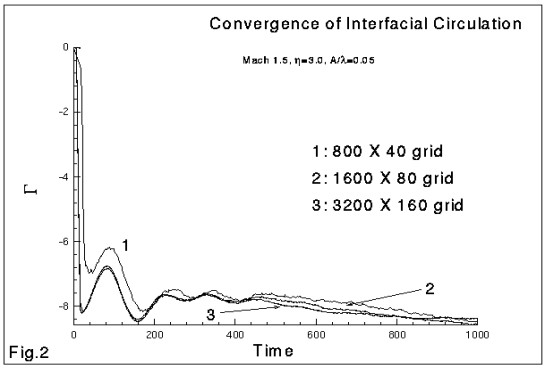

Fig.2

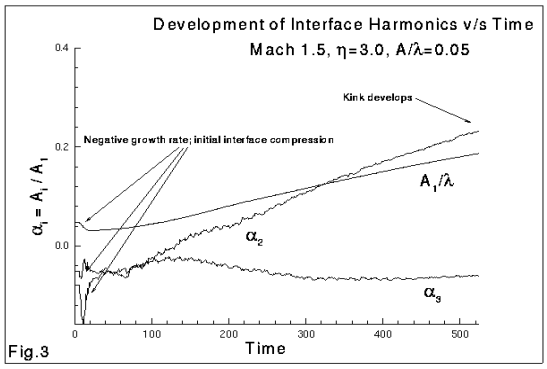

Fig.3

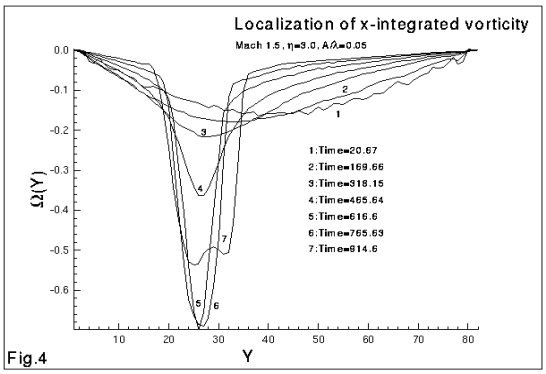

Fig.4

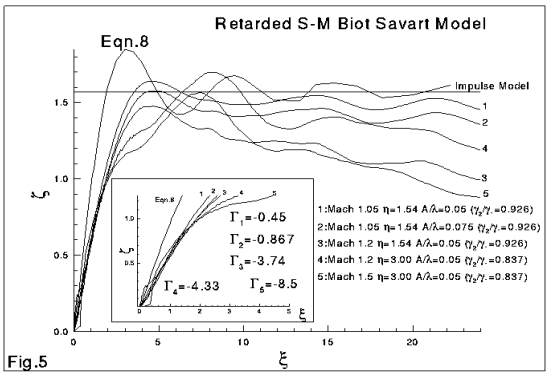

Fig.5

2 Governing Equations, Numerical Methods, Parameters and Convergence

2.1 Numerical methods

Consistent with previous numerical studies, we employ the 2D compressible Euler equations. We track the interface using a level-set method [4]. The numerical method is a second–order accurate Godunov scheme based on Chern's method [5] and is similar to the Eulerian MUSCL scheme.

The physical domain is a rectangular shock tube. The governing parameters are M, η and Ak. The undisturbed incident gas is initialized with unit pressure and density and the shock is initialized by density and pressure jumps in accord with the Rankine-Hugoniot conditions (Fig. 1 at $t = 0$).

The test gases are Air-CO_2 ($\eta = 1.54, \gamma_0 = 1.4, \gamma_b = 1.297$), Air-R_{22} ($\eta = 3.0, \gamma_0 = 1.4, \gamma_b = 1.172$), and Air-SF_6 ($\eta = 5.04, \gamma_0 = 1.4, \gamma_b = 1.0935$).

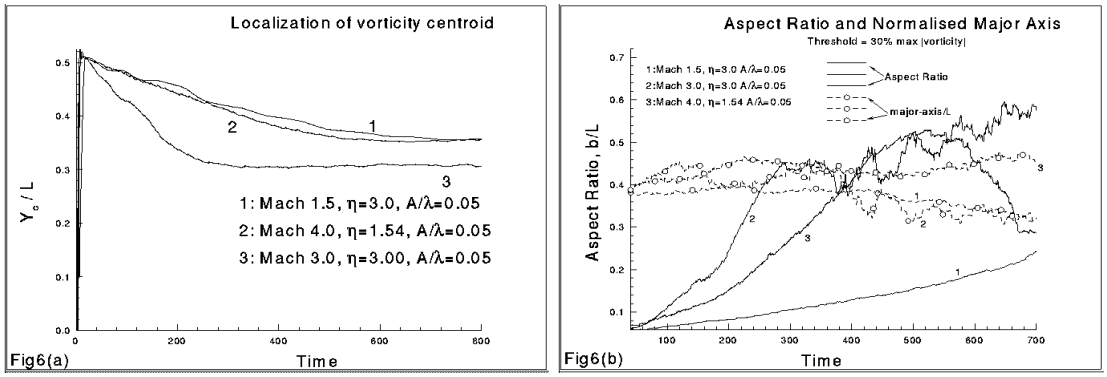

2.2 Convergence of Interfacial Circulation

In Fig. 1, we used a 1600×80 grid with $\Delta x = \Delta y = 1$.The parameters of the simulation were $M = 1.5$, $\eta = 3.0$ and $A/\lambda = 0.05$. The results are shown in Fig. 1–7. The circulation was quantified by interface-tracking procedures [3]. The results in Fig.2 show excellent convergence of interfacial *circulation* in this time domain for the last two grid sets.

3 Vortex Models

3.1 Reduced Modeling

We propose reduced models — analytical and numerical — based on an *incompressible* Biot-Savart formulation. The analytical models involve many simplifications and are less accurate; the numerical models require a minimal amount of numerical information from the simulation. In either case, the growth rate is defined as half the difference of velocities of the x-extrema of the interface.

3.2 Qualitative Aspects

After shock passage, the subsequent variation of Γ of the deposited vortex sheet are caused by secondary compression waves sweeping over the evolving interface. The magnitude of the secondary interactions are an increasing function of (M, η, Ak).

With time, higher harmonics of the perturbation become significant (Fig. 3); later the interface assumes a mushroom (spike-bubble) structure and the vorticity collapses into a patch. (Figs. 1,3.2). The localization of an unstratified vortex sheet has been studied extensively [9]: the rate of collapse and non-linearity are a function of $\Gamma(M, \eta, A)$ (Fig. 5). The $y_{centroid}$, normalized major-axes and aspect ratios of fitted ellipses, characteristic of the localization, are shown in Fig. 6.

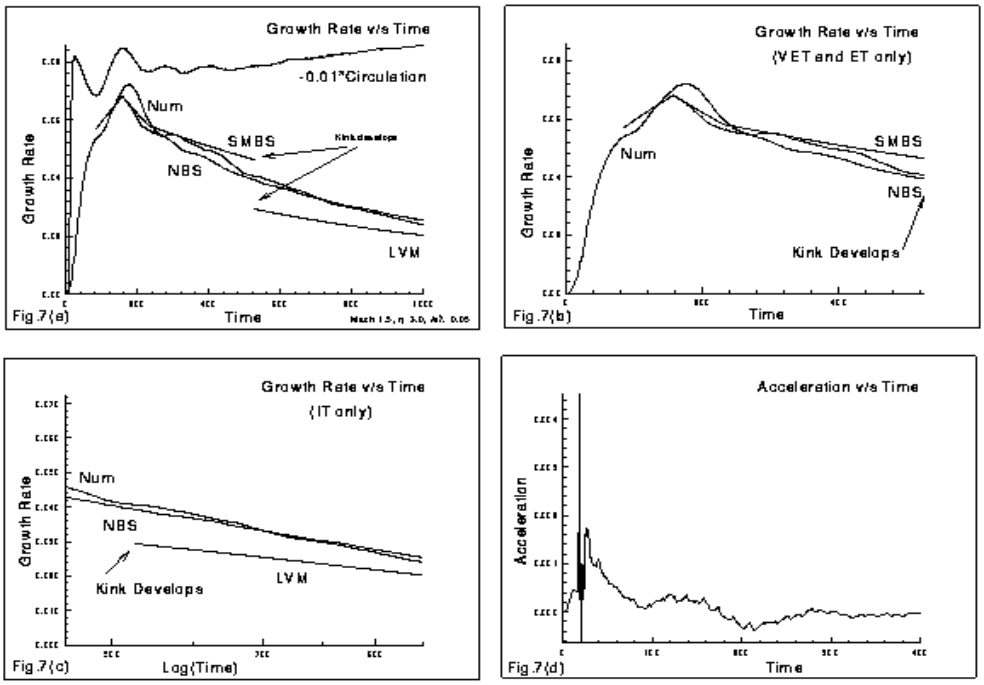

The evolution can conveniently be split into four regimes (Fig. 5); (1)Very Early Time (VET), when the incident shock and dominant compression waves sweep over the interface for the first time, i. e. approximately three shock traversal times; (2) Early Time (ET), when the evolution can be modeled by an evolving vortex sheet on a nearly incompressible interface; (3) Intermediate Time (IT), when the sheet / layer localizes into a compact structure, e. g. when the contact discontinuity becomes a multivalued function of y ; (4) Late Time (LT), when the evolution is nearly incompressible and driven by turbulent like collection of vortices. The transition times depend specifically on the details of the run.

The models for VET and ET employ a stratification-modified ansatz. The growth rate derived from a Biot-Savart formulation is corrected by $2\sqrt{\eta}/(\eta+1)$, a factor which appears in the growth rate of a perturbation on a uniform vortex sheet located on a stratified interface [7].

3.3 Numerical Biot-Savart Model (NBS)

We use this to validate the assumption of incompressibility. We integrate the instantaneous vorticity distribution over the instantaneous interface shape – both extracted from the numerical simulation – to obtain the interface growth rate.

3.4 Reduced Biot-Savart Model (SMBS)

This Biot-Savart-based model, applicable in ET, assumes incompressibility, a single mode representation of the perturbation and a frozen spectral content of the vorticity distribution. We get [6]

$$\begin{aligned} u(x,y,t) &= -\frac{1}{4\pi}\int_{\mathcal{S}} \frac{(y-y')\Omega(y')dy'}{|\vec{x}-\vec{x'}|^2}; \\ \dot{A} &= \frac{\Gamma(t)k}{4\pi}\int_{-\infty}^{\infty} \frac{\xi \sin\xi d\xi}{k^2A(t)^2(1-\cos\xi^2)^2+\xi^2} \end{aligned} \tag{3}$$

where $\Omega(y)$ is the x-integrated vorticity on the interface and $\xi = ky$.

To capture the initial growth rate, $\Gamma(t)$ is obtained by linearly interpolating between $\Gamma(t_1)$ and $\Gamma(t_2)$ for $t_1 \le t \le t_2$, $\Gamma(t_2)$ and $\Gamma(t_3)$ for $t_2 \le t \le t_3$ and $\Gamma(t) = \Gamma(t_3)$ for $t \ge t_3$, where $\Gamma(t_i)$ are the numerical (simulation) values of interfacial circulation at times of the first three local extrema after the shock has crossed the interface.

3.5 The Retarded, Stratification-Modified Biot-Savart Model (RSMBS)

We derive a model for VET from SMBS under the assumptions of $M \sim 1$ and $Ak \ll 1$; consequently the secondary interactions are negligible and $\Gamma(t) \sim const.$ We will approximate the circulation on the interface by the first term of the sine expansion for circulation on a sinusoidal interface [3]. The effect of compressibility is introduced with a retarded time, as in aeroacoustics ([10], [11]), — i. e. velocity is given by the B-S law with retarded time.

$$u(x,y,t) = -\frac{1}{4\pi}\int_{\mathcal{S}} \frac{(y-y')\Omega(y')H(t-r'/c_s)dy'}{|\vec{x}-\vec{x'}|^2} \tag{4}$$

where $(r')^2 = (x-x')^2 + (y-y')^2$ and c_s is the sound speed in the incident gas. For $M \approx 1$, P/ρ is almost unchanged and we take $c_s = \sqrt{\gamma}$.The growth rate is given by

$$\dot{A} = \frac{2\sqrt{\eta}}{\eta+1}\frac{\Gamma k}{4\pi}\int_{-\infty}^{\infty} \frac{\xi \sin\xi H(t-r'/c_s)d\xi}{k^2A(t)^2(1-\cos\xi^2)^2+\xi^2} \tag{5}$$

where $(kr')^2 = k^2A(t)^2(1-\cos\xi^2)^2 + \xi^2$. If $Ak \ll 1$, then $r' = c_st \sim y'$ and the expression simplifies to

$$\dot{A} = \frac{2\sqrt{\eta}}{\eta+1}(\Gamma_1' kA|_{0-})Si(\xi), \xi = kc_st = \sqrt{\gamma}kt \tag{6}$$

where $Si(\xi)$ is the Sine Integral function.

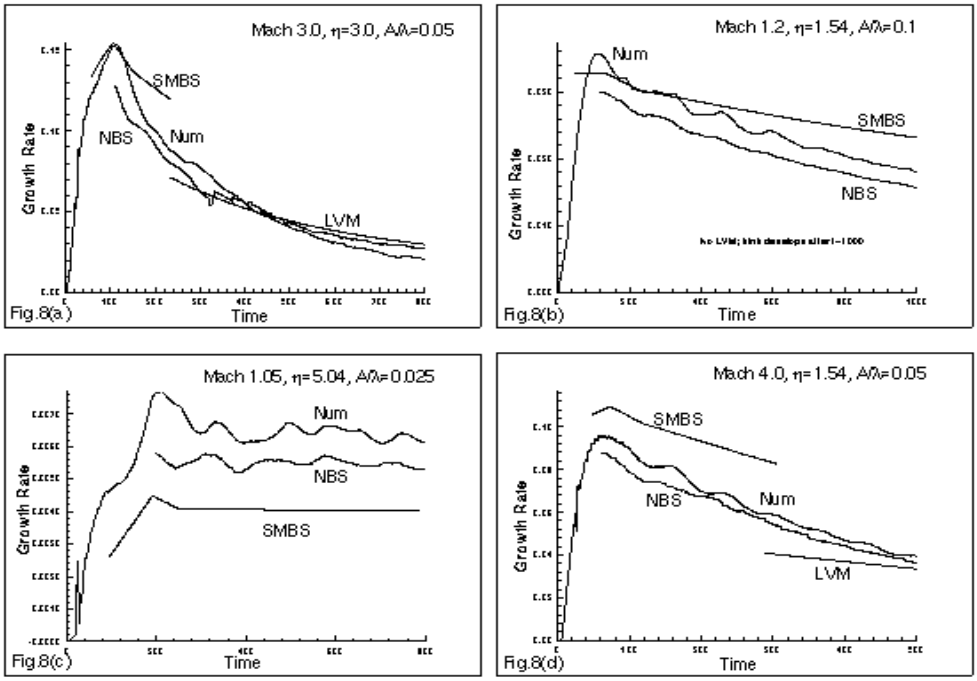

Instead of Γ_1' we use its analytical scaling result [3]

$$\Gamma_{sc} = 2\frac{\sqrt{\gamma}}{\gamma+1}(1-\eta^{-1/2})\sin\alpha(1+M^{-1}+2M^{-2})(M-1) \tag{7}$$

in Eqn. 6 to get

$$\dot{A} = \frac{4\sqrt{\gamma}}{\gamma+1}\left(1+1/M+2/M^2\right)(M-1)\frac{\sqrt{\eta}-1}{\eta+1}\frac{kA|_{0-}}{\pi}Si(\xi) \tag{8}$$

We plot $\zeta = \dot{A}/(\Gamma_{sc}A|_0 k)$ from various numerical simulations and $Si(\xi)$ versus ξ in Fig. 5. The departure from the model with increasing interfacial circulation Γ is also evident from Fig. 5.

Physically, the oscillations in $Si(\xi)$ are due to the arrival of signals from vortex images required to enforce the no–flow boundary condition, $\vec{u}.\vec{n} = 0$, at $y = 0$ and $y = \lambda/2$. As $t \to \infty$, $\dot{A} \to \dot{A}_{Richtmyer}$. Note the model does not include changes in circulation arising from secondary compressible waves, which also produce oscillatory phenomena.

3.6 The Constant–Symmetric Line Vortex Model (LVM)

This incompressible model applies at intermediate times and is analytic. We assume an array of line vortices of constant strength $(-1)^n\Gamma_L$ and location $y = (2n+1)\lambda/4, n = \ldots -2, -1, 0, 1, 2, \ldots$, where Γ_L is the first maximum in circulation and can be obtained analytically from [3].

Summing the contribution from all the vortices,

$$\dot{A} = -\frac{\beta}{\cosh kA(t)} \; ; \; or, \qquad \sinh kA(t) = -\beta kt + \sinh kA(t_s) \tag{9}$$

where $\beta = \Gamma_L k/2\pi$.

Asymptotically, Eqn. 9 approaches [6]

$$\dot{A} = \frac{\Gamma_1' kA|_0}{2\pi} \; ; \; or \qquad kA(t) = \log(-\beta kt)$$

for $Ak \ll 1$ and large times respectively.

For late time and large amplitude ($Ak \gg 1, \tanh(Ak) \approx 1$) we get

$$\dot{A} = \frac{1}{kt + C}; \qquad C = \frac{\sinh kA|_0}{-\Gamma_L k/2\pi}$$

which is similar in form to Hecht's model for v_{bubble} [12].

Note from Fig. 6 that the vorticity does not collapse into point, rather it forms a coherent structure with an aspect ratio and located at about $0.4\lambda/4$. An elliptical model should give better results.

4 Conclusion

Our vortex models provide a robust way of estimating the growth of a single mode perturbation in Richtmyer-Meshkov environments. For low Mach numbers and perturbations, there exists a simple model which tends asymptotically to the impulse model result. We expect this procedure to generalize to slow-fast cases and multiple perturbation.

In brief, the models and their applicability are

Time Regime	Models Proposed	Eqn. No.
Very Early Time	Retarded Biot-Savart (RSMBS)	6
Early Time	Sheet and Elliptical Models (SMBS, EVM)	3
Intermediate Time	Line Vortex Models (LVM)	9
Late Times	Contour Dynamical Models	

References

[1] Hawley JF, Zabusky NJ (1989) Vortex paradigms for shock–accelerated density–stratified interfaces. Phys. Rev. Lett.

[2] Richtmyer RD (1960) Taylor instability in shock acceleration of compressible fluids. Comm. Pure and Appl. Math. XIII:297

[3] Samtaney R, Zabusky NJ (1994) Circulation deposition on shock-accelerated planar and curved density stratified interfaces : Models and scaling laws. J. Fluid Mech. 269:45

[4] Mulder W, Osher S, Sethian JA (1992) Computing interface motion in compressible gas dynamics, J. Comp. Phys. 100:209

[5] Chern, I-L : *Private communication*

[6] Samtaney R, Zabusky NJ (1994) Vorticity generation and growth rate in Richtmyer–Meshkov instabilities. Caip Tech. Rept. No. 187, CAIP, Rutgers University, Piscataway, NJ-08855-1390. Submitted Phys. Flds.

[7] Chandrasekhar S (1961) Hydrodynamic and Hydromagnetic Stability. Oxford University Press.

[8] Yang Y, Zhang Q, Sharp D (1994) Small amplitude theory of Richtmyer-Meshkov instability, Phys. Fluids. 6(5):1856

[9] Pozrikidis, C and Higdon JJL(1985) Nonlinear Kelvin-Helmholtz instability of a finite layer, J. Fluid Mech. 157:225-263.

[10] Kambe, T (1986) Acoustic Emissions by Vortex Motions, J. Fluid Mech. 173:643-666.

[11] Crow, S (1970) Aerodynamic Sound Emission as a Singular Perturbation Problem, Stud. Appld. Math 49:21-44.

[12] Hecht J, Alon U, Mukamel D and Shvarts D (1994) Simple potential flow models of Rayleigh-Taylor and Richtmyer-Meshkov bubble-fronts. Tech. Rept. Preprint.

[13] Grove J, Holmes R and Sharp D (1994) Numerical Investigation of Richtmyer-Meshkov instability using Front-Tracking. LANL Rept. LA-UR-94-2024; submitted J. Fluid Mech.